

# Mesoscale eddies and their dispersive environmental impacts in the Persian Gulf

Amin Raeisi, Abbasali Bidokhti<sup>†</sup>, Seyed Mohammad Jafar Nazemosadat, and Kamran Lari

<sup>1</sup>Faculty of Natural Resources and Environment, Science and Research Branch, Islamic Azad University, Tehran 1477893855, Iran

<sup>2</sup>Geophysics Institute, University of Tehran, Tehran 1417614418, Iran

<sup>3</sup>Department of Water Engineering, Oceanic and Atmospheric Research Center, Shiraz University, Shiraz 71444165186, Iran

<sup>4</sup>Department of Physical Oceanography, Faculty of Marine Science and Technology, Tehran North Branch, Islamic Azad University, Tehran 1987973133, Iran

(Received 21 March 2020; revised manuscript received 22 April 2020; accepted manuscript online 27 May 2020)

As the mesoscale eddies in oceans and semi-enclosed seas are significant in horizontal dispersion of pollutants, we investigate the seasonal variations of these eddies in the Persian Gulf (PG) that are usually generated due to seasonal winds and baroclinic instability. The sea surface height (SSH) data from 2010 to 2014 of AVISO are used to identify and track eddies, using the SSH-based method. Then seasonal horizontal dispersion coefficients are estimated for the PG, using the properties of eddies. The results show an annual mean of 78 eddies with a minimum lifetime of one week. Most of the eddies are predominantly cyclonic (59.1%) and have longer lifetimes and higher diffusion coefficients than the anti-cyclonic eddies. The eddy activity is higher in warm seasons, compared to that of cold seasons. As locations with high eddy diffusion coefficients are high-risk areas by using maps of horizontal eddy diffusion coefficients, perilous times and locations of the release of pollutants are specified to be within the longitude from 51.38°E to 55.28°E. The mentioned areas are located from the Strait of Hormuz towards the northeast of the PG, closer to Iranian coast. Moreover, July can be considered as the most dangerous time of pollution release.

**Keywords:** Persian Gulf, mesoscale eddies, marine pollution, horizontal eddy diffusion coefficient

**PACS:** 47.27.em, 92.20.Ny, 92.10.ak, 66.10.C-

**DOI:** [10.1088/1674-1056/ab96a3](https://doi.org/10.1088/1674-1056/ab96a3)

## 1. Introduction

The Persian Gulf (PG) is a shallow semi-enclosed area located at 48–56°E and 24–30°N (Fig. 1(a)).<sup>[1]</sup> This area is extended to the delta of rivers in Iraq and Iran from the north and to a vast desert along the coasts of Qatar, Kuwait, Saudi Arabia, Bahrain, and the United Arab Emirates from the south.<sup>[2]</sup> The PG is connected to the Oman Sea through the Strait of Hormuz with a width of about 56 km.<sup>[3]</sup> The length of the PG is approximately 1000 km in the NW-SE direction, and its width varies from 56 km in the Strait of Hormuz to 338 km.<sup>[4]</sup> The lengths of the northern and southern coasts are about 1260 km and 1740 km, respectively, and the total length of the PG coasts is about 3000 km. The approximate area and volume of the PG is 239000 km<sup>2</sup> and 8780 km<sup>3</sup>.<sup>[2]</sup> The PG is the third largest gulf in the world following the Gulf of Mexico and Hudson Bay. The average depth of the PG is about 35 m, and its maximum depth has been observed to be 120 m near the Strait of Hormuz.<sup>[4]</sup> In the offshore areas, the average depth is 50–80 m. The typical depth in the coastal areas is 18–20 m, and depths of more than 40 m can be observed in some areas, especially on the Iranian coasts.<sup>[3]</sup> The depth of the PG increases from west to east and suddenly increases from the Strait of Hormuz onwards and creates depths of 200–300 m.<sup>[4]</sup> The PG bed in the north has a relatively steep slope (175 cm/km), while its slope is lower (35 cm/km) in the south.

Trough line minimum of the PG is near the Iranian coasts and extends to the coasts of the Musandam Peninsula after passing through the Tonb and Faroe islands in the Strait of Hormuz. Circulation in the PG is firstly the result of the prevailing northwesterly winds, buoyancy forcing due to high evaporation (relative to water inputs from rivers and precipitation), and the effect of tides.<sup>[5]</sup> In the first half of the year, water with a higher level of salinity can be observed in the PG.<sup>[6,7]</sup> The PG produces very salty water that flows through the Strait of Hormuz to the Oman Sea.<sup>[8]</sup> Overall, water circulation in the PG can be categorized into two main groups: (1) large-scale circulation that is mainly anti-clockwise water circulation in the basin, and (2) water circulation in the form of mesoscale eddies (Fig. 1(b)).<sup>[9]</sup> It should be mentioned that transfer of energy is from large- to small-scale motions just as the case in the cascade process and vice versa. Figure 1(b) demonstrates the development of a series of mesoscale eddies based on the model results as well as model-data comparisons.<sup>[9]</sup> The mentioned figure provides a new schematic of the PG circulation over the period of August–November. The current of Iranian coast experiences baroclinic instability after entering the PG from the Strait of Hormuz and becomes mesoscale cyclonic eddies (CE1, CE2, CE3, CE4), which are recognized as Iranian Cyclonic Eddies (ICE).<sup>[9]</sup> Blue shades also show upwelling along the Iranian coasts.<sup>[9]</sup> The blue arrows and streamlines indicate the flows of low salinity water en-

<sup>†</sup>Corresponding author. E-mail: [bidokhti@ut.ac.ir](mailto:bidokhti@ut.ac.ir)

tering the PG, which are mainly surface flows and often have mesoscale eddies formed by baroclinic instability.<sup>[9]</sup> While the red arrows and lines are the path of deep high salinity water exiting the PG.<sup>[9]</sup> Hence, the two flows represented by blue and red arrows are at two different depths.<sup>[9]</sup> According to observations and simulations in the PG, northwesterly winds usually blow intensely and prevent further penetration of the incoming water (blue) into the north, and as a result, saline water (red) on the bed also moves southeastward in the region.<sup>[9]</sup> As CE4 is more confined to the northeastern part of the PG by three coasts, it has been recognized as a weaker cyclonic eddy (a less energetic eddy or region) in a number of studies including Reynolds' <sup>[10]</sup> study.<sup>[9]</sup>

In a rotating fluid, eddies can be generated as a result of a number of processes including (1) an interaction between flows with obstacles such as oceanic flows and islands that leads to formation of eddies behind these islands, (2) a collision between two opposite flows, and (3) instabilities such as barotropic and baroclinic instabilities that generate mesoscale eddies.<sup>[11]</sup> In fluid dynamics, turbulence is a chaotic state of fluid movement. A turbulent flow is characterized by some eddies that have a wide range of the smallest to the largest size scales. A small-scale turbulence is three-dimensional while a large-scale geophysical one is quasi-two-dimensional, which mostly comprises large eddies. In such cases, flows recalculating patches of fluid have closed streamlines embodied in the main flow. Such semi-two-dimensional eddies are found in the geophysical flows such as large scale motions in the ocean and atmosphere and are strongly affected by rotation.

Expansion of a cyclonic eddy leads to upwelling of water at the center.<sup>[1]</sup> The mentioned phenomenon results in upwelling of the cold and nutrient-rich subsurface water to the surface of the water column, which results in an increase in the level of phytoplankton and other tracers. Anti-cyclonic eddies indicate a downwelling activity in their centers and are considered as eddies with a warm center as well as low biomass. Oceanic eddies have a certain lifetime ranging from several weeks to months, even reaching several years in some cases. Their maximum horizontal and vertical expansions are usually about 100 and one kilometers, respectively.<sup>[11]</sup> Accordingly, given such an aspect ratio, eddies usually have a two-dimensional pattern although smaller eddies might well grow beneath the thermocline.<sup>[11]</sup> The velocity of the expansion of eddies resembles that of the linear baroclinic waves though they are slower and have smaller widths.

Oceanic mesoscale eddies are not only significant from a dynamic point of view, but they are also important in terms of marine biochemistry and air-sea interactions.<sup>[12]</sup> Eddies are formed as a part of the balance of cycles in nature.<sup>[12]</sup> Moreover, they are the reasons for the transfer of active and passive tracers in the ocean.<sup>[11]</sup> The latter includes biochemical tracers

and pollutants, in which eddies can function collectively.

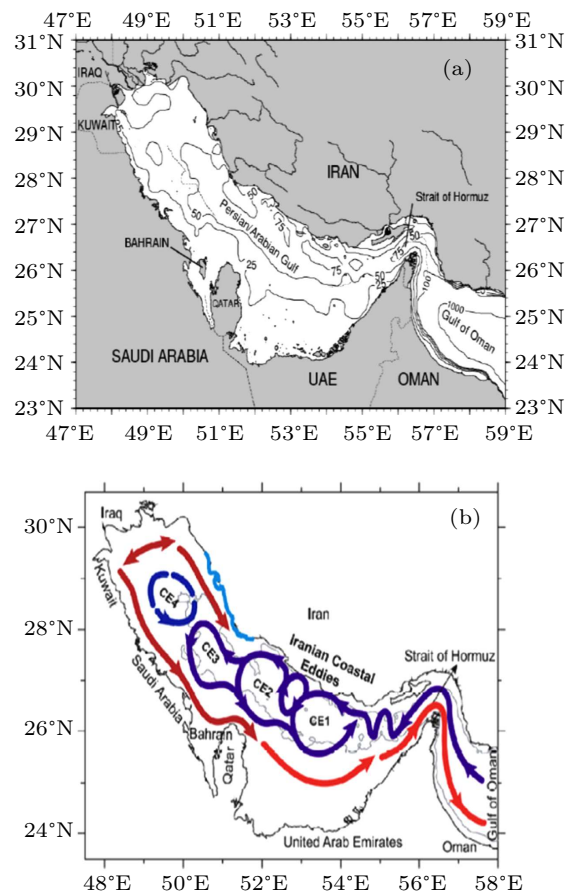


**Fig. 1.** (a) Map of the Persian Gulf region based on ETOPO2 data, depth in terms of meters.<sup>[4]</sup> (b) Water circulation in the Persian Gulf from August to November.<sup>[9]</sup>

Eddies play an important role in the transfer of kinetic energy, heat, salinity, and other tracers in the sea.<sup>[12]</sup> As warm or cold water transferred by mesoscale eddies can change the temperature and distribution of salinity, they can even significantly change the profile structure of sound speed, so they also affect the propagation of sound underwater.<sup>[13]</sup> Temperature, salinity, and pressure gradients generated by mesoscale eddies can also change the structure of the sound speed in the ocean.<sup>[13]</sup>

When eddies exchange water slantwise across a front, they perform in an advective manner, result in the creation of baroclinic instability, and make tracers to move convectively.<sup>[12]</sup> Physical conditions can be locally changed by the dynamics of eddies, as a result, reactive tracers such as phytoplankton can be directly or indirectly affected. They can also either strengthen or restrict the environmental factors for the growth of phytoplankton.<sup>[12]</sup>

The PG is a route of a number of oil tankers carrying oil from this region to other parts of the world. As the release of pollutants into the marine environment is detrimental and can result in enormous environmental and economic damages, it is of crucial significance to analyze the role of factors such

as mesoscale eddies in the estimation of pollution dispersion in the PG. Moreover, the present study can be regarded to be significant due to the fact that there are only a few studies addressing the incidents related to phenomena such as oil pollution in the ecosystem of the PG, which is susceptible to a wide range of oil release accidents because of the existence of substantial oil resources. Qualitative evaluation of the likelihood of such incidences as well as the consequences of the damages in the PG has hardly ever taken into account the potential role of eddies in this regard. Moreover, up to date, the conducted studies in this respect have only revealed the nature of cyclonic circulation in the PG.<sup>[1–3,14–17]</sup> Nonetheless, they did not precisely take into account the details of circulation in this semi-enclosed sea.<sup>[9]</sup> Yao and Johns<sup>[4]</sup> used satellite images and implemented circulation model in the PG to point out the existence of eddies in this area.

Similarly, Thoppil and Hogan<sup>[9]</sup> devoted some parts of their study to the examination of eddies using satellite images. Likewise, in another study conducted by Torabi Azad *et al.*,<sup>[5]</sup> the structure of eddies near the northern coasts of the PG was examined by collecting data using field measurements and observations. Sabetahd Jahromi *et al.*<sup>[18]</sup> explored the effect of mesoscale eddies on the distribution of temperature and salinity gradients in the PG and Strait of Hormuz. Hegarete *et al.*<sup>[8]</sup> used altimetry data to present the structure and possible recurrence of sub-mesoscale PG water fragments, in particular those embedded in mesoscale eddies. Concerning the transport and release of oil-related pollution, tracing method has been employed in most of the conducted studies including Mackay *et al.*,<sup>[19]</sup> Huang,<sup>[20]</sup> and Lonin,<sup>[21]</sup> all of which focused on surface motion of oil spots. In another study by Haj Rasouli *et al.*,<sup>[22]</sup> the movement route of pollutants and their distribution in the PG were examined considering the role of physical processes such as wind and tides in this regard. Hence, identification of the possible areas with accumulated pollutants (high-risk areas) seems to be of great value.

In this research, eddies of the PG were studied using the SSHA (sea surface height anomaly) method and AVISO reference series data from 2010 to 2014. Eddies with the lifetime of more than one week were identified and traced, and their dynamic characteristics and horizontal eddy diffusion coefficient were examined. As compared with other methods such as Okubo–Weiss parameter, the SSHA is more effective in the identification of eddies and provides more precise results in shallow areas<sup>[23]</sup> such as the PG. Another advantage of the SSH-based method is the elimination of the problematic noise from the second derivatives of SSH in the Okubo–Weiss parameter.<sup>[23]</sup> Another standard method used for the identification of eddies is the P-Delta method, which only specifies the center position of eddies and does not provide any more

information about the eddies.<sup>[23]</sup> In the SSH-based method, the points identified in the SSH curves as relative extremes are identified as the center of the eddy, and the largest SSH closed contour in the periphery of extremum point is regarded as the external eddy boundary. To analyze eddy dynamics, it is assumed that the geostrophic approximation is applicable, and eddies are assumed to have a Gaussian symmetric structure. Then, the tracking operation can be performed. The mentioned method is very identical to the SSH method that was used by Fong and Morrow<sup>[24]</sup> and Chaigneau and Pizarro,<sup>[25]</sup> with the exception that there is no need to set a threshold contour.<sup>[23]</sup> It is noteworthy that the periods over which powerful eddies appear have been identified as risky time intervals. Moreover, the distribution map of the horizontal eddy diffusion coefficient in the PG in different seasons was plotted using ArcGIS software. The areas with the highest eddy diffusion coefficient were identified as high-risk areas. The area of the mentioned regions as well as the geographical location of their center was calculated. Although previous studies using the numerical method have already been carried out regarding the identification of eddies in the PG, this is the first study that employed the SSHA method to precisely trace and identify eddies and their dynamic characteristics over four seasons. For example, Thoppil and Hogan<sup>[9]</sup> conducted an informative study that addressed eddies over a warm season using the numerical method and compared the obtained results with satellite imagery. Considering the limited number of studies carried out in the field of mesoscale eddies and their effects on the circulations of PG, the present study can provide crucial information in this respect by examining eddies in horizontal dispersion and consequently can lead to optimization of the response process regarding the spread of released pollutants in the PG. The results of the present study revealed the optimal time and location for installation of equipment and pollution disposal floats given the knowledge regarding the high-risk areas, thereby reducing economic and environmental problems in the PG.

## 2. Eddy tracking

### 2.1. SSH-based eddy tracking method

To date, a large number of eddies have been identified and tracked in SSH fields of the AVISO reference series data using automated procedures.<sup>[23]</sup> In the SSH-based method, the lines of the geostrophic flows present around eddies are considered to be approximately corresponding to the SSH closed contours. Each pixel comprises the four nearest neighboring pixels (north, south, east, and west). Within each region, there is a local maximum (minimum) point, which is the largest (smallest) of all the nearest neighboring pixels.<sup>[23]</sup> The amplitude of each cyclonic eddy is considered as the difference between the highest SSH within the eddy ( $h_{\max}$ ) and the mean

height of the outermost SSH closed contour ( $h_0$ ):<sup>[23]</sup>

$$A = h_{\max} - h_0. \quad (1)$$

Similarly, the amplitude of each anti-cyclonic eddy is considered as the difference between ( $h_0$ ) and the lowest SSH within the eddy ( $h_{\min}$ ):<sup>[23]</sup>

$$A = h_0 - h_{\min}. \quad (2)$$

The average geostrophic velocity around each SSH contour is also calculated using the following equation:<sup>[23]</sup>

$$u = -\frac{g}{f}h_y, \quad (3)$$

$$v = \frac{g}{f}h_x. \quad (4)$$

In the process of tracking, the size of each eddy is specified by its effective radius ( $L_{\text{eff}}$ ), which is the radius of a circle with the same area as that of the surrounded region around the eddy, and the eddy is considered to have a Gaussian symmetric structure.<sup>[23]</sup> After identifying each eddy and its center as the SSH geometrical center, the identified eddy is searched within the outermost closed contour area at time  $k$ , and then the mentioned process is repeated at time  $k + 1$  to find the nearest eddy in the search area until the tracking process is ceased and completed by disappearing of the eddy.

## 2.2. Eddy diffusion coefficient

As previously indicated, eddies are the result of the vertical motion of fluid and are usually caused by instability of the flows. The main characteristic of the eddy motion is the eddy diffusion coefficient, which is used to show the mixing power of turbulent flows.

Imagine a tracer following the equation<sup>[11]</sup>

$$\frac{D\varphi}{Dt} = \nabla \cdot (k_m \nabla \varphi), \quad (5)$$

where  $k_m$  is molecular diffusion. If advection flow is decay-free, molecular diffusion can be ignored. We have

$$\frac{D\overline{\varphi}}{Dt} = \nabla \cdot \overline{\varphi'v'}. \quad (6)$$

If eddy transfer is parameterized by the diffusion equation, then we will have the following equation:

$$\mathbf{F} = \nabla \overline{\varphi'v'} = -k\nabla \varphi, \quad (7)$$

where  $k$  stands for diffusion coefficient. If the focus is turned to the horizontal transfer of a tracer in  $y$ , then we can reach the equation

$$\overline{\varphi'v'} = k^{xy} \frac{\partial \overline{\varphi}}{\partial y}, \quad (8)$$

where  $k^{xy}$  denotes eddy diffusion tensor components.<sup>[11]</sup>

Assuming that eddies are the result of baroclinic instability, it can be supposed that the mixing length provided by the first deformation radius is the same as the horizontal length scale of the instability characteristic. The simplest assumption is that the velocity of eddy should be regarded as approximately equal to the magnitude of the average flow velocity  $\bar{u}$ . Hence,

$$k^{xy} \sim L_d \bar{u}, \quad (9)$$

where  $L_d \sim l'$  denotes the characteristic turbulence length.<sup>[11]</sup>

## 2.3. Data analysis

In this study, the eddy detection process was performed over five years using the SSH data of the  $1/4^\circ \times 1/4^\circ$  version obtained from the AVISO reference series. The mentioned data was filtered in seven-day steps.<sup>[23]</sup> It should be noted that the SSH and horizontal eddy diffusion coefficient maps are plotted using ArcGIS software. The method employed to study eddies in the present research was sea surface height anomaly (SSHA), which is proved to be effective in the case of using satellite data. In the SSHA curves, points denoting relative extremum are identified as eddy centers, and the largest SSHA closed contour in the periphery of extremum point is regarded as the external eddy boundary. To analyze eddy dynamics in this method, it was assumed that geostrophic approximation is applicable, through which eddy center movement, eddy boundary points, and consequently eddy advancement velocity were measured, thereby leading to the eddy tracking operation. Furthermore, eddy diffusion coefficient was measured using accessory programs.

## 3. Results

### 3.1. Mesoscale eddies

The density difference in water masses and main large-scale flows as well as surface wind turbulence leads to inclined isopycnal lines and baroclinic-instability in the Arvand flow, especially in the entrance of water from the Oman Sea into the PG, as a consequence, eddies are formed on the periphery of the main flow. Due to the formation of the thermocline and the flow of Arvand water and the water inlet of the Oman Sea to the PG through the Strait of Hormuz, required conditions are provided for the formation of mesoscale eddies, especially on the Iranian coast.<sup>[9]</sup> The entrance of less saline water into the PG through the Strait of Hormuz causes sloping density field, which is prone to baroclinic instability process. The mentioned process leads to quasi-two-dimensional turbulence that is one of the primary mechanisms governing the formation of eddies and brings about changes in not only the general water circulation in the PG but also the formation of eddies.<sup>[23]</sup>

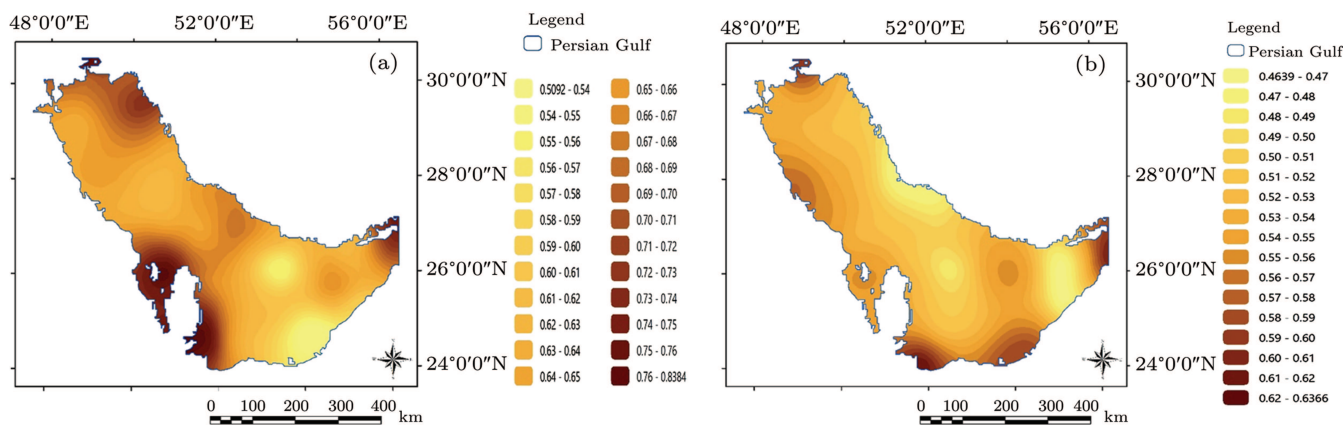


Fig. 2. Height contours in the Persian Gulf for various seasons on (a) 19 August 2014 and (b) 12 February 2014.

The results of the present study were related to eddies from 2010 to 2014 over different seasons. Figure 2 presents the map of height contours in the PG for one sample day of summer and winter of 2014. Eddies are well-demonstrated in the maps. The illustrated graphs for 2010–2014 show eddies according to the SSHA. An average of 78 eddies were observed annually (Fig. 3). It is seen that 59.1% of the observed eddies were cyclonic, and the rest were anti-cyclonic (Table 1). Given the graphs and the presented analyses, the average number of eddies as well as their histograms in several months of 2010–2014 are provided in Fig. 3. As shown, the number of eddies over summer months was more than that of the other seasons.

Table 1. Percentage of the seasonal mean of eddies considering the polarity (2010–2014).

	Spring	Summer	Autumn	Winter	Total
Cyclonic	62.10%	58.60%	55.90%	60.90%	59.10%
Anti-cyclonic	37.90%	41.40%	44.10%	39.10%	40.90%

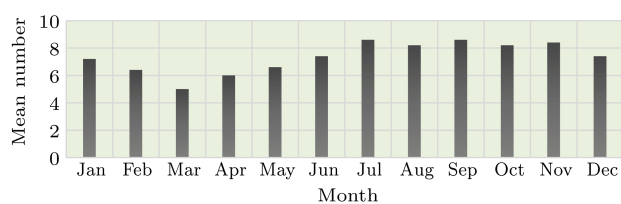


Fig. 3. Histogram of the mean number of eddies in different months from 2010 to 2014.

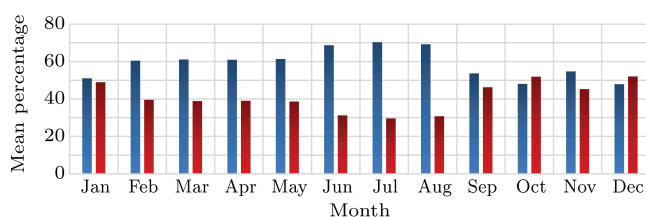


Fig. 4. Percentage of the monthly mean of eddies considering their polarity (2010–2014) (the red and blue histograms are assigned to anti-cyclonic and cyclonic eddies, respectively).

Numerical predominance of cyclonic eddies over anti-cyclonic ones was observed over all seasons, especially spring

and summer. The highest percentage of cyclonic eddies was observed in summer and July (Table 1 and Fig. 3). Since the beginning of October and the start of the autumn, the number of eddies decreased; however, the relative percentage of anti-cyclonic eddies increased, continued until January, and then decreased again (Fig. 4). As it is demonstrated, the number of eddies from July to September was more than those of any other seasons of the year.

The number of eddies increased in the early summer and winter; whereas the number of eddies decreased as the end of these seasons approached. The mentioned trends reversely occurred in autumn and spring. As already mentioned, turbulent eddies require an energy source to survive and grow. If the energy source is large enough to create instability, eddies will also be sufficiently active. One of the energy sources for the creation of instability is the potential energy stored in the sloping isopycnal lines, which can be released due to baroclinic instability.<sup>[5]</sup>

### 3.2. Calculation of horizontal eddy diffusion coefficient

This section presents the changes of horizontal eddy diffusion coefficient over different seasons within the PG area. Table 2 provides information regarding eddies with the highest diffusion coefficient  $k^{xy}$  in each season of 2014 along with the date of occurrence, polarity, radius, and their lifetimes. In Table 2, eddies of 2 (winter), 14, and 32 (autumn) are anti-cyclonic while the rest are cyclonic. As shown, the former had a lower radius and diffusion coefficient than the latter.<sup>[7]</sup>

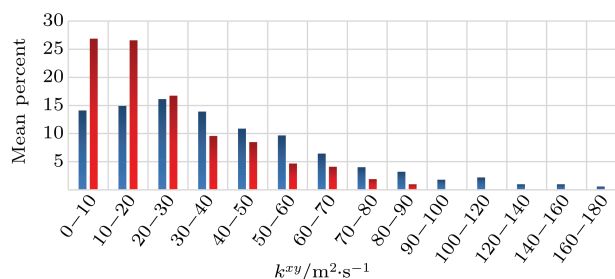
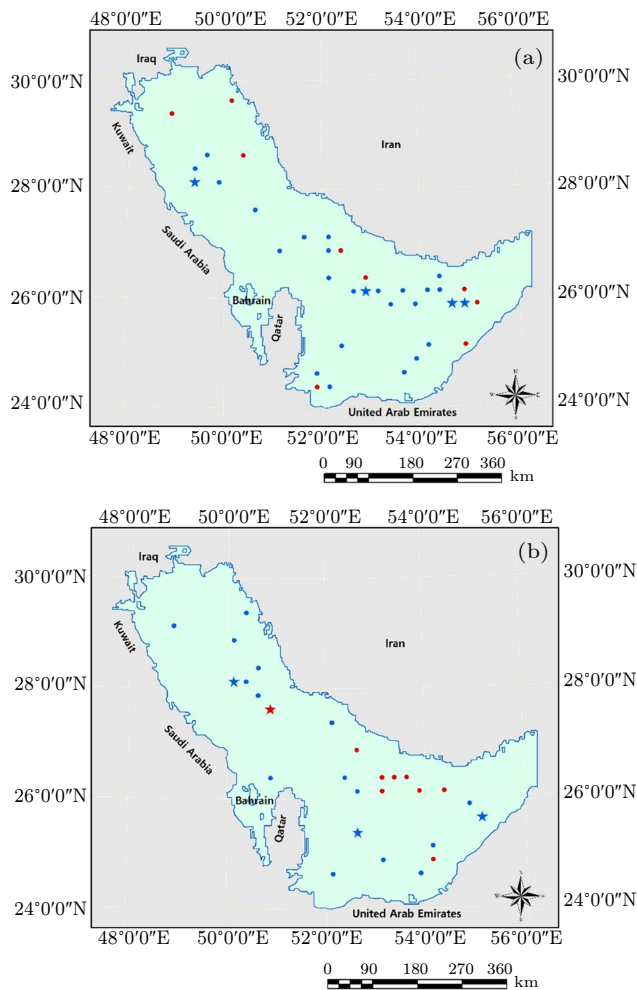


Fig. 5. The dispersion histogram of the percentage of the mean of eddy diffusion coefficient over a tensile interval (the red and blue histograms are assigned to the anti-cyclonic and cyclonic eddies, respectively).

Similar trends have been observed over other years. On average, more than 67% of the anti-cyclonic eddies had a diffusion coefficient of less than 30 (m<sup>2</sup>/s), and their maximum diffusion coefficient was 83 (m<sup>2</sup>/s). Furthermore, 42% of the cyclonic eddies had a diffusion coefficient of less than 30 (m<sup>2</sup>/s), and their maximum diffusion coefficient was 176 (m<sup>2</sup>/s) (Fig. 5 and Table 2).

**Table 2.** Eddies with the highest diffusion coefficients  $k^{xy}$  (2014).

Season	Number of eddies	$L_{eff}/\text{km}$	$k^{xy}/(\text{m}^2/\text{s})$	Lifetime/week	Date of event
Winter	20	102.95	76.70	1	26 February
	2(AC)	105.27	54.2	1	25 December
	18	65.79	53.15	3	5 March
	21	73.88	52.33	1	26 February
Spring	21	48.34	87.25	3	3 June
	21	85.59	82.68	3	27 May
	24	52.79	69.35	1	10 June
	13	49.86	62.85	1	6 May
Summer	4	53.79	116.81	4	15 July
	3	95.69	108.67	2	8 July
	1	102.42	108.09	2	15 July
	9	60.12	107.01	6	2 September
Autumn	5	77.80	79.11	3	21 October
	34	63.14	72.53	1	23 December
	14(AC)	57.51	69.93	4	2 December
	32(AC)	47.25	68.08	1	23 December



**Fig. 6.** Maps showing the place of eddies in winter (a) and summer (b) 2014 (the cyclonic and anti-cyclonic eddies with the highest diffusion coefficient are represented by five-pointed blue and red stars, respectively).

Hence, anti-cyclonic eddies, as compared with cyclonic ones, had a less significant impact on pollution dispersion (Fig. 5). In general, summer eddies were more significant in terms of spatial and temporal distribution of pollutants. Figure 6 shows where eddies occurred in the summer and winter of 2014. Cyclones, anti-cyclones, and eddies with the highest diffusion coefficient can be identified by blue, red, and five-pointed stars, respectively. In all seasons, majority of eddies were observed in the east and north of the PG.

### 3.3. High-risk areas prone to oil pollution

Pollution in PG is mainly oil pollution and its products. In areas where the diffusion coefficient is higher, the mentioned pollutants are dispersed in larger areas of the environment in a given time, thereby cleaning up oil pollution becomes more difficult. Given the mentioned point, these areas can be recognized as high-risk areas. The horizontal eddy diffusion coefficients from 2010 to 2014 were studied in different seasons. The interpolated map of the diffusion coefficient is observed across the PG over five years (Fig. 7).

As it was previously mentioned, strong eddies occurred in summer, as a result of which the interpolated maps of eddy diffusion coefficient in summer (2010–2014) were plotted to identify the high-risk areas (Fig. 7). In the mentioned maps, the areas with the highest eddy diffusion coefficients are indicated by dark color. The geographical area, geographical center, and the mean value of the coefficients of these areas were calculated (Table 3).

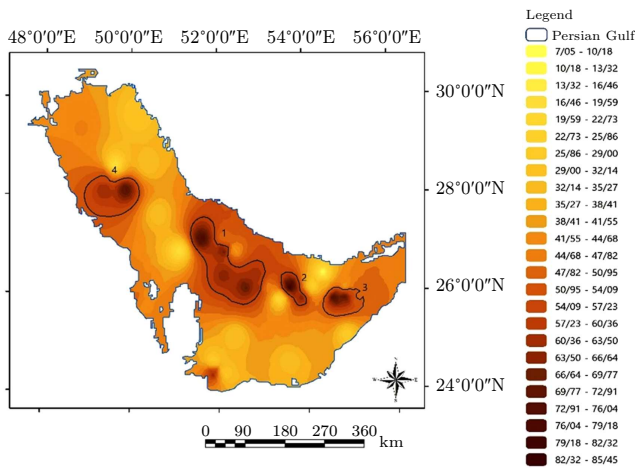


Fig. 7. The contour maps showing eddy diffusion coefficients in summer (2014) (the high-risk areas are marked with a number).

The high-risk areas in Fig. 7 were identified by numbers

Table 3. Areas of eddy occurrence along with the mean of diffusion coefficients in summer (2014).

Number of area	Area/km <sup>2</sup>	The mean of diffusion coefficient in the target area/(m <sup>2</sup> /s)	Location			
			Longitude/degree		Latitude/degree	
			from	to	from	to
1	15220.99	78.05	25.78	27.57	51.38	53.82
2	2443.09	76.02	25.74	26.42	53.42	53.98
3	4573.55	70.08	25.51	26.1	54.37	55.28
4	3901.59	65.23	27.57	28.40	48.92	50.21

### 4. Discussion

The Oman Sea water flows into the PG through the eastern areas of the PG while the most saline body of water in the PG sinks and exits in the southeastern area near the Strait of Hormuz. Moreover, Arvand flows collide with those of the PG in the northwestern areas of the PG. The mentioned process has led to the baroclinic instability, which has consequently caused the formation of eddies along the salinity fronts.<sup>[26]</sup> The penetration of the salinity front in the PG is more widespread in the summer and is prone to baroclinic instability (with a high density stratification) in warm seasons and formation of cyclonic and anti-cyclonic eddies with a peak in July and August.<sup>[26]</sup>

In other studies using numerical simulations, for instance, Thoppi and Hogan,<sup>[9]</sup> similar mesoscale eddies have also been predicted to be along the frontal system between the inflow and outflow to the PG using numerical simulations. In Figs. 8(a) and 8(b), the maps extracted from the simulation of mesoscale eddies by Thoppi and Hogan<sup>[9]</sup> (2010) and those of the present study are compared. As it is shown, maps relating to 8 July 2014 provided by the present study (right) closely, temporally, and spatially resembled the maps relating to 6 July 2005 extracted from simulations (left) provided by Thoppi and Hogan<sup>[9]</sup> (Fig. 8(a)). Such proximity and consistency between the two studies are also observed in the maps of 12 August 2014 (right) and 6 August 2005 (left) (Fig. 8(b)).

The study found that eddies located at the inlet of the PG from the Strait of Hormuz and the north of the PG were the

strongest eddies having the highest activity during July and August and were then weakened from the beginning of autumn. The results of studies conducted by Pous *et al.*<sup>[2]</sup> and Rahnemania *et al.*<sup>[26]</sup> were very close to the mentioned findings. In comparison with other eddies, they contributed more to the transmission and diffusion of pollutants because of their high diffusion coefficient. This finding was consistent with the results of other studies of such as Haj Rasooliha *et al.*<sup>[22]</sup>

The present study revealed that eddies located in the north and south of the PG are often moving towards the west and east of the PG, respectively. The mentioned finding is in line with findings presented by researchers including Rasooliha *et al.*<sup>[22]</sup> Thus, eddies in the north of the PG would distribute the pollutants first along the coast of Iran, then along the southern coasts, and finally towards the southeast of the PG. The largest area covered by eddies was the inlet of the PG from the Strait of Hormuz towards the coast of Iran and the northwest of the PG. Thus, the ecosystems of the mentioned areas are at the highest risk for distribution of pollutants in case of release.

The coastal currents from Iranian coasts to the northwest of the PG that are caused due to the existence of stronger winds during July and August can also spread oil slicks along the coasts of Iran.<sup>[26]</sup> The areas with the highest risk of spreading pollutants were within the latitude from 25.5°N to 27.57°N and the longitude from 51.38°E to 55.28°E. The contaminated areas develop fast, especially by the oil industry that makes them more prone to oil pollution.

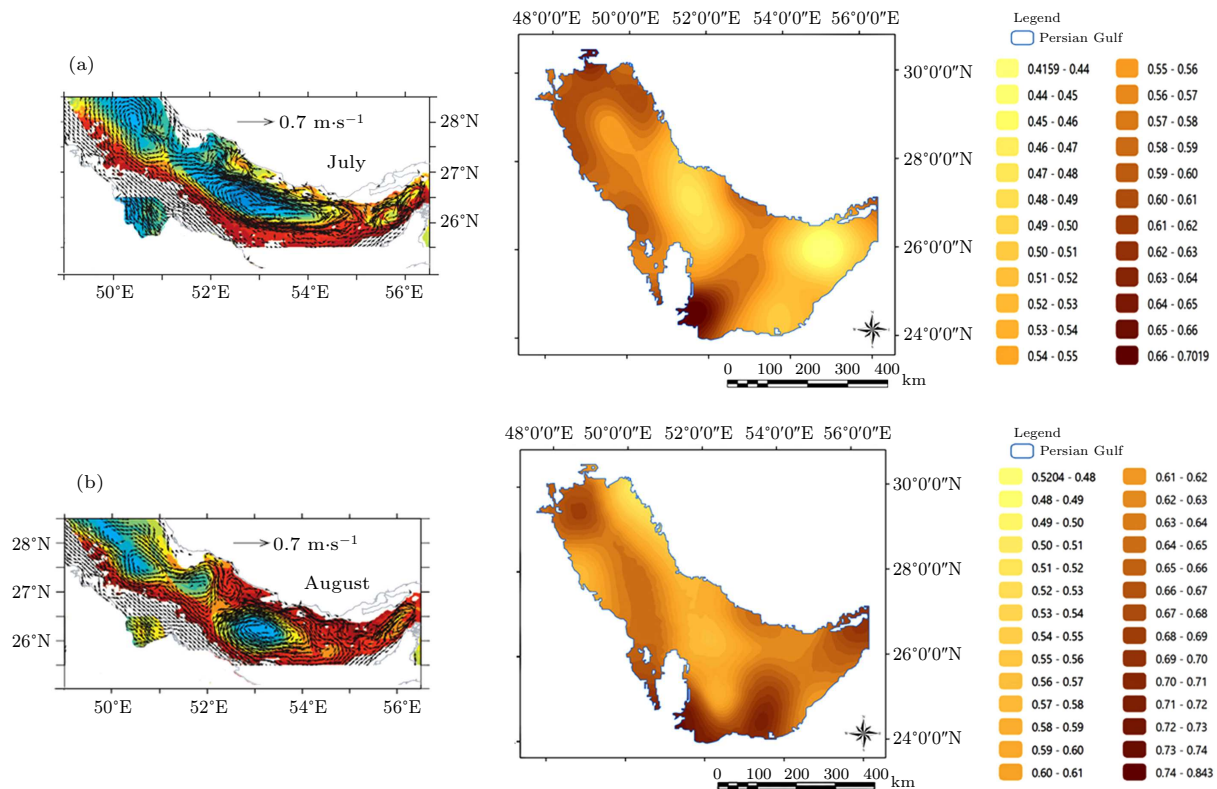


Fig. 8. (a) and (b) Maps extracted from simulations provided by Thoppil and Hagan<sup>[8]</sup> (left) and SSH maps plotted based on AVISO data (right).

Meandering currents in the circulation along the coast can also spread the oil slicks in a wider band of the Iranian coastline.<sup>[27]</sup>

## 5. Conclusions

Averagely 78 eddies per year, of which 59.1% were cyclonic, were observed throughout 2010–2014. The predominance of the number of cyclonic eddies was observed throughout the year, especially during the warm seasons. Moreover, although the anti-cyclonic eddies strengthened over the cold seasons, the mentioned trend was maintained. The horizontal eddy diffusion coefficient was also higher in summer as compared with cold seasons. The highest coefficient with the value of 176 m<sup>2</sup>/s was observed in July. The highest eddy diffusion coefficients in these seasons were related to cyclonic eddies; however, the cyclonic eddies weakened with the onset of autumn, and the anti-cyclic eddies indicated the highest diffusion coefficient in December. As the cyclonic eddies of the region, as compared with the anti-cyclonic eddies, mainly have a longer lifetime and higher horizontal eddy diffusion coefficient, they play a more significant role in the distribution of pollutants in the PG.

The present study also indicates that July and August were the highest-risk months concerning the time of eddy occurrence and distribution of pollutants. The findings also show that the eastern and northern parts of the PG have the highest eddy diffusion coefficient in the longitude from 51.38°E to 55.28°E over these months and are identified as the most risky

areas in terms of the distribution of pollutants.

Likewise, the maximum number of eddies was observed in July, whereas the minimum number of eddies in the PG was observed in May and November. The maximum number of eddies was observed in the first months of summer and winter, while the minimum number of eddies was observed in the first months of spring and autumn. Although more higher resolution measurements are required to get a more comprehensive insight regarding the distribution of mesoscale and sub-mesoscale eddies in the PG and the impacts of eddies on marine pollutant dispersion, the results of the present study can be used as a guide to prioritize the skimming processes and estimate the possible damages to this unique marine ecosystem considering the likelihood of the occurrence of various scenarios of pollution release and their consequences.

## References

- [1] Chao S Y, Kao W T and Al-Hajiri K R 1992 *J. Geophys. Res.* **97** 11219
- [2] Pous S, Lazure P and Carton X 2015 *Cont. Shelf Res.* **94** 55
- [3] Kämpf J and Sadrinasab M 2006 *Ocean Sci.* **2** 27
- [4] Yao F and Johns W E 2010 *J. Geophys. Res.* **115** C11017
- [5] Torabi Azad M, Banazadeh Mahani M and Bidokhti A A 2000 *J. Environ. Sci. Technol.* **10** 17
- [6] Bower A S, Hunt H D and Price J F 2000 *J. Geophys. Res.* **105** 6387
- [7] Johns W E, Yao F and Olson D B 2003 *J. Geophys. Res.* **108** 3391
- [8] Hegarete, P L, Carton X, Louazel S and Boutin G 2016 *Ocean Sci.* **12** 687
- [9] Thoppil P G and Hogan P J 2010 *J. Phys. Oceanogr.* **40** 2122
- [10] Reynolds R M 1993 *Mar. Pollut. Bull.* **27** 35
- [11] Vallis, G K 2005 *Atmospheric and Oceanic Fluid Dynamics* (Cambridge: Cambridge Press) Chap 10 p. 450



- [12] Frengner I, Münich M, Gruber N and Kutti R 2015 *J. Geophys. Res.: Ocean* **120** 7413
- [13] Xiao Y, Li Z, Li J, Liu J and Sabra K 2019 *Chin. Phys. B* **28** 054301
- [14] Blain C A 2000 *The 6th International Conference. American Society of Civil Engineers* (New York, USA) p. 74
- [15] Bidokhti A A and Ezam M 2009 *Ocean Sci.* **5** 1
- [16] Ezam M, Bidokhti A A and Javid A H 2010 *Ocean Sci.* **6** 887
- [17] Noori R, Abbasi M R, Aamowski J F and Dehghani M 2017 *Estuarine Coastal Shelf Sci. (ECSA)* **197** 236
- [18] Sabetahd Jahromi A A, Lari K, Sultani M and Raeisi A 2011 *The 13th Marine Industry Conference* (Kish, Iran 8–10 November 2011) p. 249
- [19] Mackay D, Peterson S and Nadeau S 1980 *National Conference on Control of Hazardous Material Spills* (Louisville, USA 13–15 May 1980) p. 364
- [20] Huang J C 1983 *Proceeding of the 1983 Oil Spill Conference* (Washington DC, USA 28 February–3 March 1983) p. 313
- [21] Lonin S A 1999 *Spill Sci. & Tech. Bull.* **5** 331
- [22] Haj Rasouliha O, Hasanzadeh E and Rezaei Latifi A 2013 *J. Climatology Res.* **15** 93
- [23] Chelton D B, Schlax M G and Samelson R M 2011 *Prog. Oceanogr.* **91** 167
- [24] Fang F and Morrow R 2003 *Deep-Sea Res.* **50** 245
- [25] Chaigneau S, Gizolme A and Grados C 2008 *Prog. Oceanogr.* **79** 106
- [26] Rahnama, A, Bidokhti A A, Ezam M, Lari K and Ghader S 2019 *J. Appl. Fluid Mech.* **12** 1475
- [27] Raeisi A, Bidokhti A A, Nazemosadat S M J, Lari K and Sabetahd A A 2017 *The 19th Marine Industry Conferences* (Kish, Iran 11–13 December 2017)